Effect of Solar Concentration on the Thermodynamic Power Conversion Efficiency of Quantum-Dot Solar Cells Exhibiting Multiple Exciton Generation

ARTICLE *in* JOURNAL OF PHYSICAL CHEMISTRY LETTERS · OCTOBER 2012

Impact Factor: 7.46 · DOI: 10.1021/jz301077e

3 AUTHORS, INCLUDING:

Matthew C Beard
National Renewable Energy Laboratory
114 PUBLICATIONS **7,874** CITATIONS
SEE PROFILE

A. J. Nozik
University of Colorado Boulder
310 PUBLICATIONS **19,501** CITATIONS
SEE PROFILE

THE JOURNAL OF PHYSICAL CHEMISTRY Letters

Letter

pubs.acs.org/JPCL

Effect of Solar Concentration on the Thermodynamic Power Conversion Efficiency of Quantum-Dot Solar Cells Exhibiting Multiple Exciton Generation

Mark C. Hanna,[†] Matthew C. Beard,*[,†] and Arthur J. Nozik*[,†,‡]

[†]Center for Advanced Solar Photophysics, Chemical and Materials Sciences Center, National Renewable Energy Laboratory, Golden, Colorado, United States

[‡]Department of Chemistry and Biochemistry, University of Colorado, Boulder, Colorado, United States

Supporting Information

ABSTRACT: Thermodynamic calculations show that all solar cells can convert solar photons into electricity or fuel with higher theoretical power conversion efficiencies under concentrated sunlight. For conventional (viz, present day) single-junction solar cells that produce at most one electron−hole pair per absorbed photon, the theoretical increase in efficiency is relatively small (absolute values of 38% at 500× vs 33% at 1×). However, when solar concentration is combined with multiple exciton generation (MEG) in semiconductor quantum dots, the increase in theoretical power conversion efficiency is greatly enhanced. For the ideal MEG case, where the threshold for exciton multiplication is twice the bandgap, E_g, the maximum thermodynamic efficiency increases to 75% at 500×, but the optimum E_g shifts to smaller values. If E_g is fixed at the 1-sun optimal level, then the maximum theoretical efficiency still increases markedly, becoming 62% at 500× for the staircase MEG characteristic (defined as producing N electron−hole pairs when the photon energy is $N \times E_g$) and 47% for a linear MEG characteristic that has a threshold photon energy of $2E_g$. The bandgaps in these two cases are 0.70 and 0.93 eV, respectively.

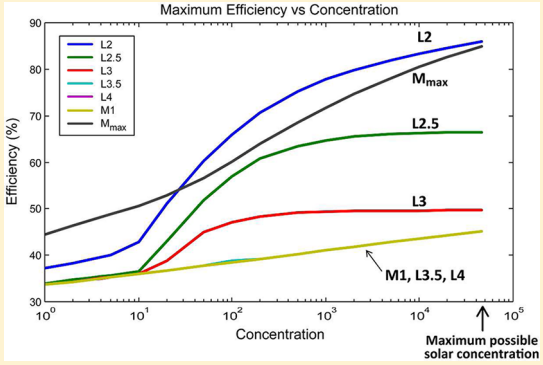

SECTION: Energy Conversion and Storage; Energy and Charge Transport

It is well known that the use of solar concentration can increase the theoretical power conversion efficiency (PCE) of photovoltaic solar cells.[1−3] Thus, for example, with no concentration (1-sun intensity) the maximum possible PCE for conventional single-junction PV cells is calculated from the Shockley−Queisser (S−Q) thermodynamic analysis to be 31−33% (depending upon the AM1.5 solar spectrum selected for the calculation).[4] This S−Q calculation is based on several assumptions in addition to the 1-sun intensity: (1) the only loss of photogenerated electrons and positive holes (charge carriers) is through radiative recombination (this is termed the radiative limit); (2) detailed balance is assumed; (3) a maximum yield of one electron−hole pair (EHP) per absorbed photon is produced; (4) photons less than E_g are not absorbed, and (5) thermal equilibrium is attained between electrons, holes, and phonons. The resulting maximum possible PCE occurs for solar cells using semiconductors with bandgaps (E_g) between about 1.2 and 1.4 eV. At a concentration of 500 suns, the PCE increases to 38%, and at 1000 suns (the present practical technological limit), it becomes 40%.[1] The maximum possible terrestrial solar concentration is 46 300 suns, at which level of concentration the maximum PCE becomes 45%.

The important assumption of the initial S−Q analysis that each absorbed photon produces just one EHP (hereafter labeled the M1 case) can be eliminated under certain situations;[5,6] this can lead to much higher theoretical PCEs depending on the details of the EHP multiplication process.[7,8] One such situation shown by recent theoretical and experimental work is that in solar cells based on semiconductor nanocrystals (NCs) where at least one dimension is small enough to experience quantum-confinement, more than one EHP can be created per absorbed photon.[9−11] In general, the minimum photon energy required to initiate EHP multiplication is twice the semiconductor bandgap (or HOMO−LUMO in molecular terminology) and is only limited by energy conservation; in principle, N EHPs can be produced from photons that have energies N times E_g. In bulk semiconductors, crystal momentum must also be conserved;[12,13] this additional constraint increases the required photon energy to begin the process of EHP multiplication from single photons. For parabolic bands, the excess energy ($\Delta E_{ex} = h\nu - E_g$) for an electron to undergo multiplication is $\Delta E_e = (2m_e^* + m_h^*)E_g/(m_e^* + m_h^*)$, where m_e^* is the effective mass of the electron and m_h^* is the effective mass of the hole. For bulk

Received: July 31, 2012
Accepted: September 17, 2012
Published: September 17, 2012

   dx.doi.org/10.1021/jz301077e | J. Phys. Chem. Lett. 2012, 3, 2857−2862

PbSe, where $m_e^* \approx m_h^*$, the excess energy needed in both the conduction and valence bands is therefore, $3E_g/2$ and because, in this case, the excess energy is equally divided between the electron and hole ($\Delta E_{ex} = \Delta E_e + \Delta E_h$), the photon energy needed to achieve this required excess energy is $4E_g$. The exact threshold energy depends on the specific band structure, and the competing channel of hot-exciton cooling must also be considered and therefore should be determined for each material of interest. The importance of band structure in determining the threshold for EHP multiplication in bulk Si and Si−Ge alloys was discussed in ref 12 ,where a threshold of about 4 eV was reported for bulk Si. However, in NCs exhibiting quantum confinement, the requirement to satisfy crystal momentum is relaxed because momentum is not a good quantum number. For example, in PbSe QDs the threshold photon energy is $\sim 3E_g$, below the allowed onset for bulk PbSe, experimentally measured at $5E_g$.[14] Ideally, the minimum photon energy for EHP multiplication can approach $2E_g$ and leads to highly efficient EHP production. There are several examples in the literature where this limit is being approached, most notably in arrays of Si QDs[15] and carbon nanotubes.[16]

S−Q-type calculations[7,8] for the PCE of solar cells based on the use of semiconductor NCs where EHP multiplication is possible for photon energies $\geq 2E_g$ show that the maximum PCE at 1-sun can be increased to ~40% relative to the 1 EHP/photon (M1) cell, depending on the threshold photon energy and efficiency of the EHP process. Furthermore, when EHP multiplication is combined with solar concentration, the maximum possible PCE values are dramatically increased compared with conventional solar cells with no EHP multiplication, reaching values that can be nearly twice that of conventional solar cells (e.g., 78 vs 40% at 1000 suns). The relative increase depends on E_g, the EHP multiplication threshold energy, and the solar concentration level. All of these factors and their influence on maximum possible PCE are also presented below.

Multiple Exciton Generation in Nanocrystals. Quantization effects develop in semiconductor NCs when electrons and holes in these materials become confined by potential barriers to very small regions of space. The NC size at which quantization effects become important depends on the effective mass, the electronic structure of the semiconductor material, and the Bohr radius of excitons in the bulk, but this size typically ranges from 2 to 20 nm. The confinement can be in one dimension (producing quantum films, also called 1-D quantum wells), in two dimensions (producing quantum wires or rods), or in three dimensions (producing what is termed quantum dots (QDs)).

Spatial confinement of electrons and holes in NCs leads to the following effects: (1) In the lowest excited state of the NCs, the EHPs become correlated because of Coulomb interactions and thus exist as excitons rather than free carriers. (2) The rate of hot electron and hole (i.e., hot exciton) cooling can be slowed because of the formation of discrete electronic states.[17−19] (3) Momentum is not a good quantum number, and thus the need to conserve crystal momentum is relaxed.[17] (4) Auger processes are greatly enhanced because of increased Coulomb coupling.[9,18,20−23] Because of these factors, it was predicted that the production of multiple EHPs will be enhanced in NCs compared with bulk semiconductors; both the threshold energy, $h\nu_{th}$, for MEG and its efficiency, η_{MEG} (defined as the number of excitons produced per additional bandgap of energy above $h\nu_{th}$), are expected to be greatly enhanced. In NCs, we label the formation of multiple excitons multiple exciton generation (MEG); free carriers can form only upon dissociation of the excitons, for example, in various PV device structures.

The ideal MEG process produces N EHPs when the photon energy is $N \times E_g$. This produces a staircase characteristic for a plot of quantum yield (QY) versus photon energy divided by bandgap ($h\nu/E_g$), where 2 EHPs are produced at $2E_g$, 3 EHPs at $3E_g$, and so forth (labeled M_{max} in Figure 1). An indication of a staircase characteristic has been suggested in refs 24, 15, and 16. However, most MEG results to date do not show a staircase characteristic but rather a linear dependence of QY, and for these characteristics a recent analysis[8] shows that $h\nu_{th}$ and η_{MEG} are related by the simple expression

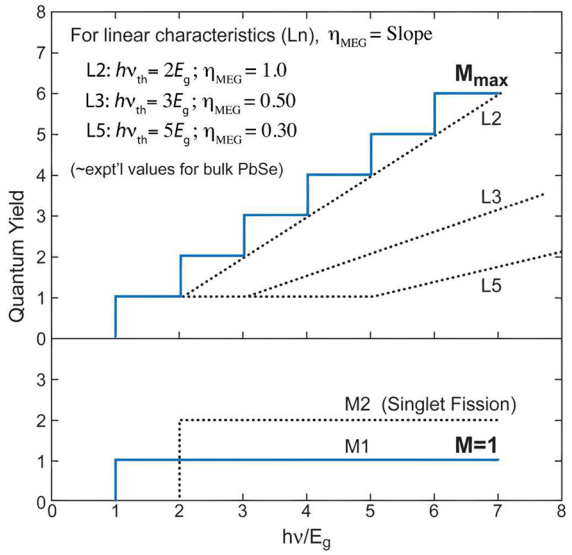

Figure 1. Possible characteristics for MEG in nanocrystals relating QY to photon energy normalized to the bandgap (E_g). There are two types of characteristics: a staircase function (labeled (M_{max}) with a threshold at $2E_g$) and a linear function where the QY is linear with normalized photon energy after the threshold for MEG is reached. The linear functions are labeled $L(n)$ where n = photon energy threshold in units of $h\nu/E_g$ and η_{MEG} = slope = MEG efficiency. The slope of this plot is defined as the MEG efficiency and is the number of additional excitons produced per additional bandgap of photoexcitation energy after the MEG threshold is reached. The characteristic for singlet fission (the molecular analog of MEG) is also shown but is not discussed here. For a review, see M. Smith and J. Michl.[27]

$$\frac{h\nu_{th}}{E_g} = 1 + \frac{1}{\eta_{MEG}} \quad (1)$$

For example, a threshold of $2E_g$ yields a MEG efficiency of 1, $3E_g$ an efficiency of 0.5, and so on. For the linear characteristic, the slope of the QY versus $h\nu/E_g$ is η_{MEG} and QY = $(h\nu/E_g - 1)\eta_{MEG}$. In the following presentation, we considered various MEG linear characteristics that are labeled $L(n)$, where L indicates that the characteristic is a linear function (not the staircase function) and n indicates the value of $h\nu_{th}/E_g$.

The staircase function can be recovered from the linear function by considering the dynamics of hot exciton MEG rates, r_{MEG}, versus cooling rates, r_{cool}. In this treatment, the threshold photon energy is given by

dx.doi.org/10.1021/jz301077e | J. Phys. Chem. Lett. 2012, 3, 2857−2862

$$h\nu_{th} = \left(2 + \frac{r_{cool}}{r_{MEG}^{2h\nu_{th}}}\right)E_g \quad (2)$$

where $r_{MEG}^{2h\nu_{th}}$ is the MEG rate at $h\nu = 2h\nu_{th}$ and r_{cool} is the cooling rate (assumed to be independent of photon energy). In our treatment, we define cooling as the process restricted to electron (or hole) phonon scattering and hence heat; MEG also results in electrons or holes relaxed to a thermalized, colder state, but this process is distinguished from cooling that involves phonons. As $r_{MEG}^{2h\nu_{th}}$ increases or r_{cool} decreases, the $h\nu_{th}$ approaches the energy conservation limit of $2E_g$. In terms of the e−h pair creation energy,[25,26] ε_{eh} (the required excess energy to produce one additional e−h pair), $h\nu_{th}$ is given by $h\nu_{th} = E_g + \varepsilon_{eh}$. The perfect staircase function can be obtained from the analysis when $r_{MEG}^{2h\nu_{th}}/r_{cool} > 10\,000$, that is, when the MEG rate is 10 000 times faster than the hot exciton cooling rate.[8]

Ultimate Thermodynamic PCE of MEG Coupled to Solar Concentration. S−Q thermodynamic PCE calculations were made for the various MEG characteristics shown in Figure 1. The results are presented in Figures 2−7. Figure 2 presents the

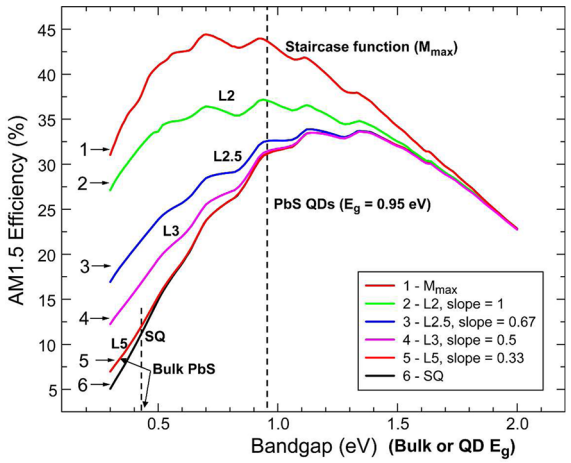

Figure 2. Power conversion efficiency (PCE) versus bandgap at 1-sun intensity ($C = 1$) for different MEG characteristics calculated using the Shockley−Queisser detailed balance thermodynamic analysis modified for exciton multiplication described by the MEG characteristic noted on the Figure. Reproduced with permission from ref 8.

S−Q calculations of PCE versus bandgap at 1-sun concentration and is reproduced from our previous analysis.[8] The maximum efficiency occurs for the staircase MEG characteristic (M_{max}), with a peak PCE of 44 to 45% for bandgaps ranging from 0.7 to 1 eV. The L2 and L2.5 characteristic also produce significant PCE gains, even at bandgaps below the optimum value, but when the threshold is $>2.5E_g$, the PCE efficiency gain at 1-sun is marginal. Therefore, for 1-sun applications it is critical to optimize the MEG process to approach the M_{max} case as closely as possible.

Figure 3 is a semilog plot of the maximum PCE as a function of solar concentration for various MEG characteristics (M_{max} and $L(n)$, n = 2, 2.5, 3, 3.5, and 4) and also for M1 (normal cell) for comparison. In this plot, the optimum bandgaps for MEG are allowed to vary for each concentration, and the peak PCE for each concentration is selected after allowing the bandgap to vary. Important features of Figure 3 are that the maximum PCE increases very dramatically with solar concentrations above 10× for MEG thresholds less than

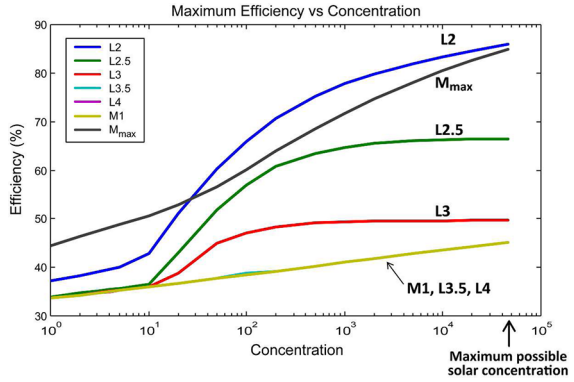

Figure 3. Effect of solar concentration on PCE for various MEG characteristics. For each concentration value, the maximum possible PCE is selected from the plot of PCE versus bandgap; bandgap is a free variable.

$2.5E_g$, becoming 75% at a concentration of 500× for the L2 characteristic; also, the PCE increase is highly nonlinear with concentration. This is in contrast with conventional solar cells (M1), which have a linear increase of PCE with the log of concentration and reach 38% at 500×. The PCE behavior for MEG cells with $h\nu_{th} > 3E_g$ is essentially the same as that for M1; this is because for $h\nu_{th}$ above $3E_g$ there is limited PCE benefit because the photon energies required for MEG are too high and mainly fall outside the solar spectrum. MEG thresholds between 2.5 and $3E_g$ yield significant gains in PCE for concentrations above 10×. Interestingly, the PCE for L2 becomes greater than that of M_{max} at 40 and then converges at a PCE of 85% for the maximum possible concentration (46 300 suns). This unexpected behavior and the nonlinearity of the MEG characteristics will be discussed below. Our results for M_{max} and L2 are consistent with previous calculations on the effect of solar concentration combined with carrier multiplication in bulk semiconductors.[28]

Figure 4 shows the PCE results for the L2 MEG characteristic as a function of bandgap for various solar concentrations; the concentration values of the various plots are 1, 2, 5, 10, 20, 50, 100, 200, 500, 1000, 2000, 5000, 10 000, 20 000, 46 300. The optimum PCE shifts very dramatically to much lower bandgaps above a concentration of 10×; the optimum bandgap range that provides the most rapidly rising

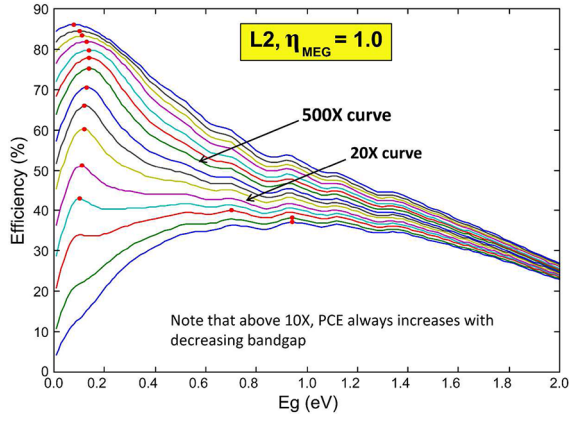

Figure 4. Optimum bandgaps (red dots) for maximum MEG PCEs for various solar concentrations of: 1, 2, 5, 10, 20, 50, 100, 200, 500, 1000, 2000, 5000, 10 000, 20 000, and 46 300 for the L2 MEG characteristic.

dx.doi.org/10.1021/jz301077e | J. Phys. Chem. Lett. 2012, 3, 2857−2862

maximum PCEs are in the range of 0.10 to 0.15 eV. Above 10×, the PCE always increases with lower bandgaps in contrast with conventional cells and MEG cells with solar concentrations below 10×, where in both cases the PCE drops at lower bandgaps. The reason for this behavior and how the PCEs can be so high for such low bandgaps is explained below.

The low bandgaps of 0.10 to 0.15 eV could be difficult to achieve in realistic applications. Thus, it is of interest to determine the behavior of PCE with solar concentration when combined with MEG at fixed bandgaps that are larger and hence more accessible. This can be readily determined from plots for any given MEG characteristic (like L2 in Figure 4) by drawing a vertical line at any given bandgap and reading off the PCEs for the efficiency plots for the various concentrations. This is done in Figure 5 for L2 characteristic for the fixed

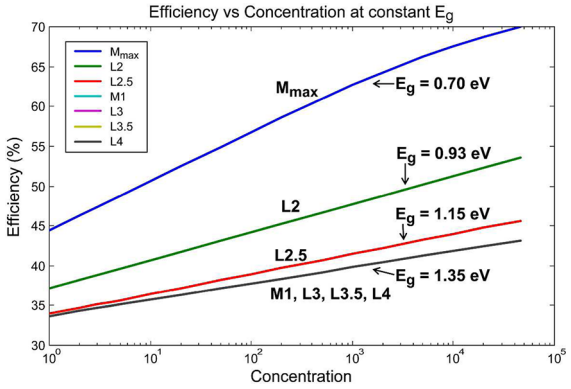

Figure 5. Efficiency versus concentration for various MEG characteristics with E_g fixed at the optimum E_g (maximum PCE) for a solar concentration of 1-sun (C = 1).

bandgaps of 0.70, 0.93, 1.15, and 1.35 eV; these bandgap values are the ones where the PCEs have a peak value in the S−Q plots of PCE versus E_g (as in Figure 2) for the different MEG characteristics of M_{max}, L2, L2.5, and M1. (M1 has equivalent PCE to $L(n)$, $n \geq 3$.) Although the gain in theoretical maximum PCE with concentration with fixed bandgaps is not as great as when the bandgap is allowed to vary with solar concentration, the PCE gains are still very substantial, especially for M_{max} and L2. In the latter two cases at 500×, the PCEs are 62 and 48%, respectively, versus 38% for M1 (no MEG).

The gain in the maximum possible PCE when MEG is combined with solar concentration is dramatic. The effect is greatest when the optimum bandgap is allowed to vary for the different MEG characteristics and concentration values, thus becoming, for example, 75% at 500× for the L2 characteristic versus 38% for a conventional solar cell at 500× with no MEG (M1 characteristic). However, the peak PCEs occurs with very low values of the bandgap (0.10 to 0.15 eV). If the bandgap is held constant with increasing solar concentration, then the possible maximum PCEs also increase substantially, reaching, for example, 62% at 500× for the M_{max} characteristic (E_g = 0.70 eV) and 48% for the L2 characteristic (E_g = 0.93 eV).

The rapid increase in PCE for low bandgaps with increasing solar concentration is caused by two effects that increase the maximum photocurrent: (1) the maximum MEG multiplication factor increases with lower bandgap because it is equal to solar photon energy divided by the bandgap and (2) at low bandgaps (0.10 to 0.15 eV) thermal energy from the environment can cause interband transitions and hence produce additional excitons added to those from optical excitation. These effects are clearly shown in Figure 6, where the short circuit

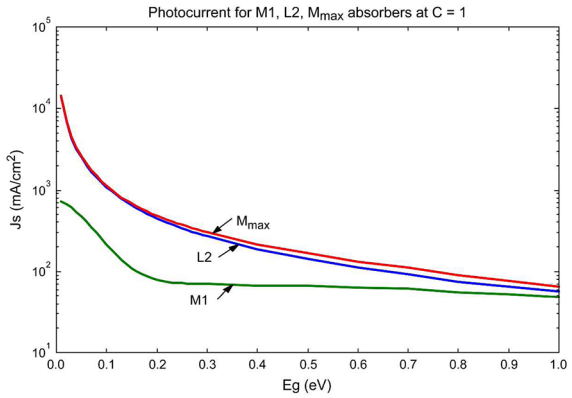

Figure 6. Short-circuit photocurrent versus QD bandgap for M1, L2, and M_{max} MEG characteristics.

photocurrent is plotted versus solar concentration for M1, L2, and M_{max}. The steep rise in photocurrent for the NC cells compared with normal cells is evident, and the former photocurrent rises even faster below 0.15 eV due to thermal excitation.

In Figure 7a, the photocurrent for L2 at the maximum operating point of a NC PV cell is plotted versus solar concentration for bandgaps of 0.1, 0.5, 1.0, and 1.5 eV. The slopes are of course linear, but the magnitude of the slope decreases with increasing bandgap. This is due to the higher MEG exciton multiplication factors for the small bandgaps that amplify the photocurrent at any concentration by the exciton multiplication factor. As a result, the photocurrent of the lower bandgap systems is much larger than the photocurrent of the larger bandgap systems, and the difference becomes increasingly greater with increasing solar concentration. In Figure 7b, the photovoltage at the maximum operating point is plotted versus the log of the solar concentration for the same four bandgaps (0.1, 0.5, 1.0, and 1.5 eV). For larger bandgap systems, the photovoltage is a logarithmic function of light intensity but is always less than the bandgap because of thermodynamic considerations. However, for systems with small bandgap, the photovoltage approaches the bandgap at high light intensity, and the logarithmic dependence breaks down. All of the above factors lead to the nonlinear plots of PCE versus log of solar concentration for NC solar cells exhibiting MEG, as seen in Figure 2; they also result in the much greater maximum possible PCE values such cells exhibit as the solar concentration increases.

In Figure 3, a nonintuitive result is that the PCE for L2 as a function of solar concentration crosses the PCE for M_{max} at a concentration of 25× and becomes larger than the PCE for M_{max} until they begin to converge at the maximum possible concentration of 46 300. This is unexpected because in Figure 2 the PCE for M_{max} is always greater than L2 at all bandgap values and at 1-sun intensity. The reason for this crossover has to do with the behavior of the photovoltage at the maximum power point for L2 and M_{max} in this region of inverted PCE values where the concentration exceeds 25× and the optimum bandgap as a function of concentration is not fixed and shifts to much lower bandgaps above 25×. The calculated current−voltage characteristics for L2 and M_{max} at a given solar concentration for the small bandgaps show that whereas the

dx.doi.org/10.1021/jz301077e | J. Phys. Chem. Lett. 2012, 3, 2857−2862

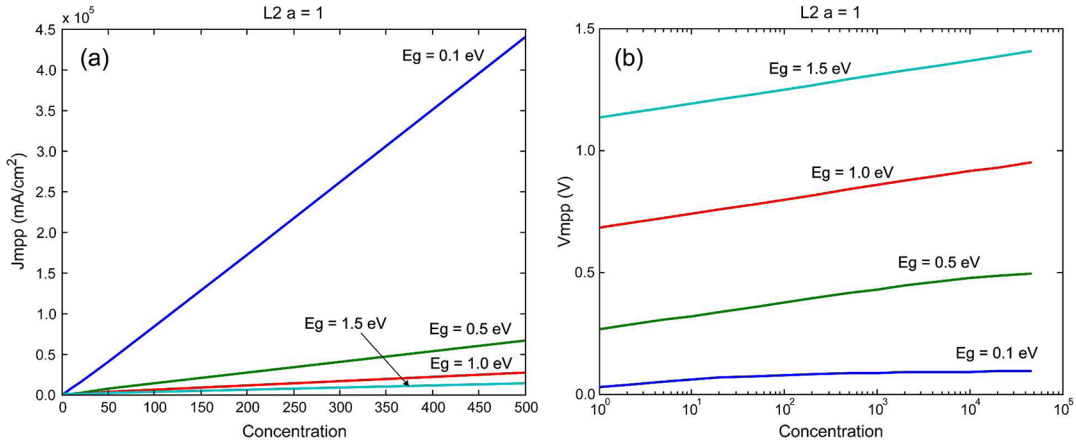

Figure 7. (a) Photocurrent at the maximum power point vs solar concentration for various QD bandgaps for the L2 characteristic. (b) Photovoltage at maximum power point vs log concentration for different QD bandgaps for the L2 characteristics.

photocurrent for M_{max} is always greater than that for L2, the photovoltage for L2 is always larger at the maximum power point yielding a higher PCE for L2. This is shown in Figure S1 in the Supporting Information for the condition of maximum solar concentration. The photovoltage for M_{max} is lower because the radiative recombination current is greater for M_{max} compared with L2, as also shown in Figure S1 in the Supporting Information.

For cases where the bandgap is fixed at the optimum PCE values at 1-sun for the MEG characteristics and the solar concentration increased (Figure 5 for M_{max} and L2), the crossover of PCE for L2 above M_{max} does not occur. This is because the optimum bandgaps under this scenario are larger, and both the photocurrent and the photovoltage for M_{max} are larger than L2.

Finally, it is of interest to note that the presence of MEG and CM in an actual QD solar cell operating under AM1.5 solar irradiation has recently been reported showing a QY for photocurrent >100% (for both external and internal QY values) for photons within the solar spectrum.[11] This is important because the determined internal QYs for photocurrent match the QYs reported by several groups based on time-resolved ultrafast transient spectroscopy for isolated QDs in colloidal solutions; the latter is a less direct method to measure exciton population that had been subjected to some controversy concerning the magnitude or even existence of MEG in QDs and its significance for potentially enhancing solar cell performance when MEG is optimized in real devices.

■ ASSOCIATED CONTENT

Supporting Information

Details retaining to calculating power conversion efficiency as well as supporting figures. This material is available free of charge via the Internet http://pubs.acs.org.

■ AUTHOR INFORMATION

Corresponding Author

*E-mail: arthur.nozik@colorado.edu; matt.beard@nrel.gov.

Notes

The authors declare no competing financial interest.

■ ACKNOWLEDGMENTS

We acknowledge support of the Center for Advanced Solar Photophysics (CASP), an Energy Frontier Research Center (EFRC) funded by the U.S. Department of Energy, Office of Science, Office of Basic Energy Sciences. DOE funding was provided to the National Renewable Energy Laboratory (NREL) through contract DE-AC36-08G028308.

■ REFERENCES

(1) Nelson, J. *The Physics of Solar Cells*; Imperial College Press: London, 2003.

(2) Reuter, H.; Schmitt, H. Efficiencies of Single and Graded Gap Solar-Cells at Terrestrial Solar Spectra. *J. Appl. Phys.* **1992**, *71*, 5957–5963.

(3) Henry, C. H. Limiting Efficiencies of Ideal Single and Multiple Energy-Gap Terrestrial Solar-Cells. *J. Appl. Phys.* **1980**, *51*, 4494–4500.

(4) Shockley, W.; Queisser, H. J. Detailed Balance Limit of Efficiency of p-n Junction Solar Cells. *J. Appl. Phys.* **1961**, *32*, 510.

(5) Green, M. A. *Third Generation Photovoltaics*; Bridge Printery: Sydney, 2001;

(6) Queisser, H. J. Multiple Carrier Generation in Solar Cells. *Sol. Energy Mater. Sol. Cells.* **2010**, *94*, 1927–1930.

(7) Hanna, M. C.; Nozik, A. J. Solar Conversion Efficiency of Photovoltaic and Photoelectrolysis Cells with Carrier Multiplication Absorbers. *J. Appl. Phys.* **2006**, *100*, 074510.

(8) Beard, M. C.; Midgett, A. G.; Hanna, M. C.; Luther, J. M.; Hughes, B. K.; Nozik, A. J. Comparing Multiple Exciton Generation in Quantum Dots To Impact Ionization in Bulk Semiconductors: Implications for Enhancement of Solar Energy Conversion. *Nano Lett.* **2010**, *10*, 3019–3027.

(9) Nozik, A. J. Quantum Dot Solar Cells. *Physica E* **2002**, *14*, 115–120.

(10) Schaller, R. D.; Klimov, V. I. High Efficiency Carrier Multiplication in PbSe Nanocrystals: Implications for Solar Energy Conversion. *Phys. Rev. Lett.* **2004**, *92*, 186601.

(11) Semonin, O. E.; Luther, J. M.; Choi, S.; Chen, H. Y.; Gao, J. B.; Nozik, A. J.; Beard, M. C. Peak External Photocurrent Quantum Efficiency Exceeding 100% via MEG in a Quantum Dot Solar Cell. *Science* **2011**, *334*, 1530–1533.

(12) Wolf, M.; Brendel, R.; Werner, J. H.; Queisser, H. J. Solar Cell Efficiency and Carrier Multiplication in Si1-xGex Alloys. *J. Appl. Phys.* **1998**, *83*, 4213–4221.

(13) Landsberg, P. T. *Recombination in Semiconductors*; Cambridge University Press: New York, 1991;

(14) Pijpers, J. J. H.; Ulbricht, R.; Tielrooij, K. J.; Osherov, A.; Golan, Y.; Delerue, C.; Allan, G.; Bonn, M. Assessment of Carrier-Multiplication Efficiency in Bulk PbSe and PbS. *Nat. Phys.* **2009**, *5*, 811–814.

(15) Trinh, M. T.; Limpens, R.; de, B., WDAM; Schins, J. M.; Siebbeles, L. D. A.; Gregorkiewicz, T. Direct Generation of Multiple

Excitons in Adjacent Silicon Nanocrystals Revealed by Induced Absorption. *Nat. Photonics* **2012**, *6*, 316−321.
(16) Gabor, N. M.; Zhong, Z. H.; Bosnick, K.; Park, J.; McEuen, P. L. Extremely Efficient Multiple Electron-Hole Pair Generation in Carbon Nanotube Photodiodes. *Science* **2009**, *325*, 1367−1371.
(17) Nozik, A. J.; Beard, M. C.; Luther, J. M.; Law, M.; Ellingson, R. J.; Johnson, J. C. Semiconductor Quantum Dots and Quantum Dot Arrays and Applications of Multiple Exciton Generation to Third-Generation Photovoltaic Solar Cells. *Chem. Rev.* **2010**, *110*, 6873−6890.
(18) Nozik, A. J. Spectroscopy and Hot Electron Relaxation Dynamics in Semiconductor Quantum Wells and Quantum Dots. *Annu. Rev. Phys. Chem.* **2001**, *52*, 193−231.
(19) Pandey, A.; Guyot-Sionnest, P. Slow Electron Cooling in Colloidal Quantum Dots. *Science* **2008**, *322*, 929−932.
(20) Shabaev, A.; Efros, A. L.; Nozik, A. J. Multiexciton Generation by a Single Photon in Nanocrystals. *Nano Lett.* **2006**, *6*, 2856−2863.
(21) Ellingson, R. J.; Beard, M. C.; Johnson, J. C.; Yu, P. R.; Micic, O. I.; Nozik, A. J.; Shabaev, A.; Efros, A. L. Highly Efficient Multiple Exciton Generation in Colloidal PbSe and PbS Quantum Dots. *Nano Lett.* **2005**, *5*, 865−871.
(22) Efros, A. L.; Rosen, M. Random Telegraph Signal in the Photoluminescence Intensity of a Single Quantum Dot. *Phys. Rev. Lett.* **1997**, *78*, 1110−1113.
(23) Klimov, V. I.; Mikhailovsky, A. A.; McBranch, D. W.; Leatherdale, C. A.; Bawendi, M. G. Quantization of Multiparticle Auger Rates in Semiconductor Quantum Dots. *Science* **2000**, *287*, 1011−1013.
(24) Timmerman, D.; Valenta, J.; Dohnalová, K.; de Boer, W.; Gregorkiewicz, T. Step-Like Enhancement of Luminescence Quantum Yield of Silicon Nanocrystals. *Nat. Nanotechnol.* **2011**, *6*, 710−713.
(25) Alig, R. C.; Bloom, S.; Sruck, C. W. Electron-Hole-Pair Creation Energies in Semiconductors. *Bull. Am. Phys. Soc.* **1980**, *25*, 175.
(26) McGuire, J. A.; Sykora, M.; Joo, J.; Pietryga, J. M.; Klimov, V. I. Apparent Versus True Carrier Multiplication Yields in Semiconductor Nanocrystals. *Nano Lett.* **2010**, *10*, 2049−2057.
(27) Smith, M. B.; Michl, J. Singlet Fission. *Chem. Rev.* **2010**, *110*, 6891−6936.
(28) Spirkl, W.; Ries, H. Luminescence and Efficiency of an Ideal Photovoltaic Cell with Charge Carrier Multiplication. *Phys. Rev. B* **1995**, *52*, 11319.